

Draft version date 2016 August 30

Einstein@Home discovery of a Double-Neutron Star Binary in the PALFA Survey

P. Lazarus¹, P. C. C. Freire¹, B. Allen^{2,3,4}, S. Bogdanov⁵, A. Brazier^{6,7}, F. Camilo⁸,
F. Cardoso⁹, S. Chatterjee⁶, J. M. Cordes⁶, F. Crawford¹⁰, J. S. Deneva¹¹, R. Ferdman^{12,13},
J. W. T. Hessels^{14,15}, F. A. Jenet¹⁶, C. Karako-Argaman^{12,13}, V. M. Kaspi^{12,13},
B. Knispel^{2,3}, R. Lynch¹⁷, J. van Leeuwen^{14,15}, E. Madsen^{12,13}, M. A. McLaughlin⁹,
C. Patel^{12,13}, S. M. Ransom¹⁷, P. Scholz^{12,13}, A. Seymour¹⁸, X. Siemens⁴, L. G. Spitler¹,
I. H. Stairs^{19,13}, K. Stovall²⁰, J. Swiggum⁸, A. Venkataraman¹⁸ W. W. Zhu¹,

arXiv:1608.08211v2 [astro-ph.HE] 31 Aug 2016

ABSTRACT

We report here the Einstein@Home discovery of PSR J1913+1102, a 27.3-ms pulsar found in data from the ongoing Arecibo PALFA pulsar survey. The pulsar is in a 4.95-hr double neutron star (DNS) system with an eccentricity of 0.089. From radio timing with the Arecibo 305-m telescope, we measure the rate of advance of periastron to be $\dot{\omega} = 5.632(18)^\circ/\text{yr}$. Assuming general relativity accurately models the orbital motion, this corresponds to a total system mass of $M_{\text{tot}} = 2.875(14) M_\odot$, similar to the mass of the most massive DNS known to date, B1913+16, but with a much smaller eccentricity. The small eccentricity in-

¹Max-Planck-Institut für Radioastronomie, Auf dem Hügel 69, 53121 Bonn, Germany; pfreire@mpifr-bonn.mpg.de

²Max-Planck-Institut für Gravitationsphysik, D-30167 Hannover, Germany

³Leibniz Universität Hannover, D-30167 Hannover, Germany

⁴Physics Dept., Univ. of Wisconsin - Milwaukee, Milwaukee WI 53211, USA

⁵Columbia Astrophysics Laboratory, Columbia Univ., New York, NY 10027, USA

⁶Dept. of Astronomy, Cornell Univ., Ithaca, NY 14853, USA

⁷Center for Advanced Computing, Cornell Univ., Ithaca, NY 14853, USA

⁸SKA South Africa, Pinelands, 7405, South Africa

⁹Dept. of Physics, West Virginia Univ., Morgantown, WV 26506, USA

¹⁰Dept. of Physics and Astronomy, Franklin and Marshall College, Lancaster, PA 17604-3003, USA

¹¹National Research Council, resident at the Naval Research Laboratory, Washington, DC 20375

¹²Dept. of Physics, McGill Univ., Montreal, QC H3A 2T8, Canada

¹³McGill Space Institute, McGill Univ., Montreal, QC H3A 2T8, Canada

¹⁴ASTRON, the Netherlands Institute for Radio Astronomy, Postbus 2, 7990 AA, Dwingeloo, The Netherlands

¹⁵Anton Pannekoek Institute for Astronomy, Univ. of Amsterdam, Science Park 904, 1098 XH Amsterdam, The Netherlands

¹⁶Center for Gravitational Wave Astronomy, Univ. of Texas - Brownsville, TX 78520, USA

¹⁷NRAO, Charlottesville, VA 22903, USA

¹⁸Arecibo Observatory, HC3 Box 53995, Arecibo, PR 00612

¹⁹Dept. of Physics and Astronomy, Univ. of British Columbia, Vancouver, BC V6T 1Z1, Canada

²⁰Dept. of Physics and Astronomy, Univ. of New Mexico, NM 87131, USA

dicates that the second-formed neutron star (the companion of PSR J1913+1102) was born in a supernova with a very small associated kick and mass loss. In that case this companion is likely, by analogy with other systems, to be a light ($\sim 1.2 M_{\odot}$) neutron star; the system would then be highly asymmetric. A search for radio pulsations from the companion yielded no plausible detections, so we can’t yet confirm this mass asymmetry. By the end of 2016, timing observations should permit the detection of two additional post-Keplerian parameters: the Einstein delay (γ), which will enable precise mass measurements and a verification of the possible mass asymmetry of the system, and the orbital decay due to the emission of gravitational waves (\dot{P}_b), which will allow another test of the radiative properties of gravity. The latter effect will cause the system to coalesce in ~ 0.5 Gyr.

Subject headings: (stars:) pulsars: general, (stars:) pulsars: individual (PSR J1913+1102), stars: neutron, (stars:) binaries: general, gravitation

1. Introduction

Studies of pulsars in double neutron star (DNS) binary systems provide exquisite tests of relativistic gravity (e.g. Kramer et al. 2006; Weisberg & Huang 2016) and binary stellar evolution (e.g. Ferdman et al. 2013); they also allowed the first and still the most precise neutron star (NS) mass measurements (Taylor & Weisberg 1982; Kramer et al. 2006). Historically, NS mass measurements were important to constrain the equation of state of ultra-dense matter (e.g. Lattimer & Prakash 2004). DNS orbits are observed to be slowly contracting due to the emission of gravitational waves (GWs), thus demonstrating their existence (e.g. Taylor & Weisberg 1982); studies of the DNS population can be used to inform the expected rate of Advanced LIGO detection NS-NS mergers (Abadie et al. 2010).

Pulsars in DNS systems are quite rare: out of ~ 2500 known radio pulsars, only 14 are known to be in DNS systems¹, including two in the “double pulsar” system, J0737–3039². See Martinez et al. (2015) for a recent summary of pulsars in DNS systems.

¹There is still some debate on the nature of the companion of two of these pulsars, PSRs J1906+0746 and J1807–2500B.

²In this work, we only use the prefix PSR when referring to individual pulsars, in the latter system PSR J0737–3039A and B. For the systems, we use the prefix DNS, unless we refer to them specifically as a binary system.

DNS systems are typically found in large-scale, un-targeted radio pulsar surveys such as the on-going Pulsar-ALFA (PALFA) survey with the 305-m William E. Gordon telescope of the Arecibo Observatory in Puerto Rico (Cordes et al. 2006). PALFA observations are focused on the two regions of the Galactic plane visible from Arecibo ($32^\circ \lesssim \ell \lesssim 77^\circ$ and $168^\circ \lesssim \ell \lesssim 214^\circ$ within $|b| < 5^\circ$) and are conducted at 1.4 GHz using the 7-beam Arecibo L-Band Feed Array (ALFA) receiver and the Mock spectrometers (for a recent overview of this survey, its observing set-up and its PRESTO-based data reduction pipeline³, see Lazarus et al. 2015). In addition to the PRESTO-based pipeline, all PALFA survey observations are analyzed using the Einstein@Home pulsar search pipeline (for details see Allen et al. 2013). The relatively short, 268-s pointings of this survey allows for the discovery of highly accelerated pulsars in compact binary systems using relatively low computational cost “acceleration” searches. A prime example is PSR J1906+0746, the first DNS system found in the PALFA survey and second most relativistic DNS system currently known (Lorimer et al. 2006; van Leeuwen et al. 2015): this system was detected with the “quicklook” pipeline without any acceleration searches.

In this paper we present the discovery and early follow-up of PSR J1913+1102, a member of a new DNS system. The paper is organized as follows: The discovery and follow-up observations are summarized in §2. §3 describes the analysis and results from timing as well as a search for radio pulsations from the companion of PSR J1913+1102. The results of these analyses are discussed in §4, this includes a discussion on the nature, eccentricity, total mass and possible mass asymmetry of this new system. Prospects for future timing observations of this binary system are presented in §5 before the paper is concluded in §6.

2. Discovery and follow-up

PSR J1913+1102 was discovered by the Einstein@Home pipeline in a PALFA observation taken on 2010 September 26 (all dates and times are in UT). The pulsar has a spin period of 27.3 ms and a dispersion measure (DM) of 339 pc cm^{-3} . For the pulse profile, the reduced χ^2 was 3.3, which corresponds to a detection significance of 8.5σ for the best acceleration ($-54 \pm 14 \text{ m s}^{-2}$). For zero acceleration, the reduced χ^2 is only 1.4, which corresponds to a significance of 5.5σ . This implies that this pulsar is in a highly accelerated binary system and that it would not have been discovered without the acceleration search algorithms.

³PRESTO can be found at <https://github.com/scottransom/presto> and the PALFA survey PRESTO-based pipeline can be found at <https://github.com/plazar/pipeline2.0>.

Following its discovery, PSR J1913+1102 was observed at the Arecibo Observatory using the ALFA receiver and Mock spectrometers using an observing set-up identical to PALFA survey observations (see Lazarus et al. 2015, for details). In short, the 322-MHz observing band centered at 1375 MHz is divided into two overlapping sub-bands. Each 172 MHz sub-band is divided into 512 channels and is sampled every $\sim 65.5 \mu\text{s}$. In this observing mode, the two linear polarizations are summed and only the total intensity is recorded. In total, 11 observations were conducted in this mode between 2012 May 25 and 2013 September 20. Integration times ranged between 110 and 1200 s.

The variations of the measured period of the pulsar in these observations established that PSR J1913+1102 is in a 4.95-hr binary orbit with an eccentricity of $e \simeq 0.09$. The mass function, $M_f \simeq 0.136 M_\odot$, yields, assuming a pulsar mass $M_p = 1.35 M_\odot$, a companion mass $M_c > 0.878 M_\odot$.

Starting on 2012 November 10, PSR J1913+1102 was also observed with the L-wide receiver at the Arecibo Observatory using the Puerto Rico Ultimate Pulsar Processor Instrument (PUPPI) backend in “incoherent” mode. These L-wide PUPPI observations contain 600 MHz of usable bandwidth centered at 1380 MHz uniformly sub-divided into 2048 channels. PSR J1913+1102 was observed with this set-up 36 times before 2014 January 1 (the cut-off for this work). All 36 PUPPI “incoherent” mode observations were phase-aligned and integrated together to form a high- S/N ($S/N = 98.7$) L-band profile of PSR J1913+1102. The resulting profile is shown in the top plot of Fig. 1. The average pulse profile has a half-power duty cycle of ~ 0.08 . It shows an exponential decay after the main pulse, as if the signal is affected by interstellar scattering; this is not too surprising given the high DM of the pulsar. This is confirmed by the fact that the exponential decay timescale becomes much longer at lower frequencies, as shown in the lower plot of Fig. 1.

A summary of the observations included in this paper is presented in Table 1. All of these observations were conducted in search mode because at the time the observations were taken we still lacked a phase-coherent timing solution that would allow for coherent

Table 1: Observation Summary

| Receiver | Data Recorder | Mode | Span (MJD) | Center Frequency (MHz) | Total Bandwidth (MHz) | No. of channels | No. Obs. | No. TOAs |
|----------|------------------|--------|---------------|------------------------------|-----------------------------|-----------------|----------|----------|
| ALFA | Mock (Low band) | Search | 56072–56555 | 1300.168 | 172.032 | 512 | 11 | 53 |
| ALFA | Mock (High band) | Search | 56072–56555 | 1450.168 | 172.032 | 512 | 11 | 55 |
| L-Wide | PUPPI | Search | 56241–56642 | 1440 | 800 ^a | 2048 | 36 | 405 |

^aThe L-wide receiver has a bandwidth of ~ 600 MHz, only that part of the band is scientifically useful.

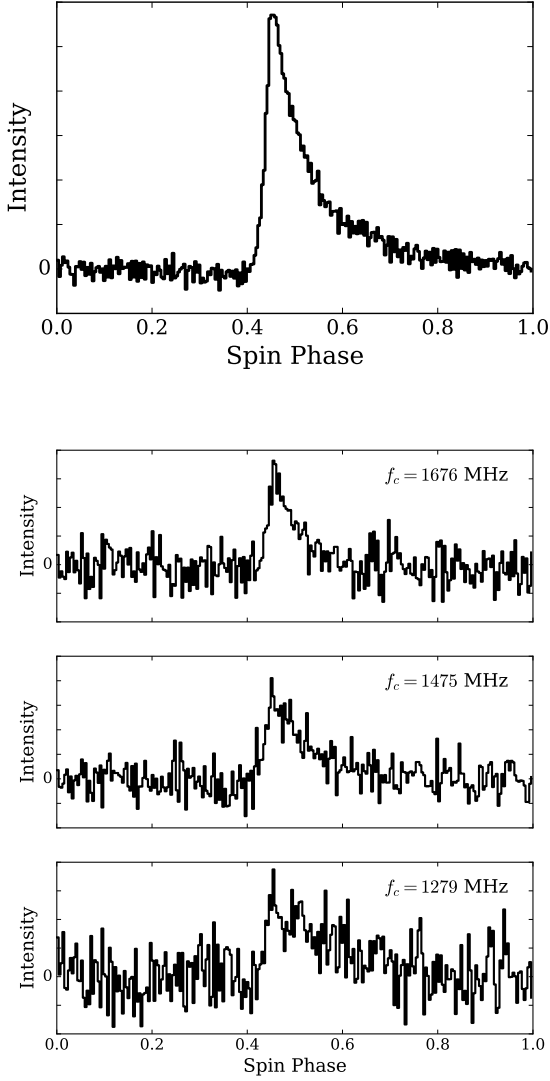


Fig. 1.— *Top*: A high- S/N ($S/N=98.7$) profile of PSR J1913+1102 at L-band (centered at 1380 MHz) created by phase-aligning and summing all 36 incoherent PUPPI observations. A total of 5.3 hr of data were summed. Details of the observing set-up used for the observations included in the profile can be found in § 2 and Table 1. The pulse profile exhibits exponential decay after the main pulse, this is likely caused by interstellar scattering, a common occurrence for pulsars at high DMs. *Bottom*: Pulse profile from one of the longest observations at three separate sub-bands. We can see here that the exponential decay becomes much longer at lower frequencies, as expected from interstellar scattering.

dedispersion and online folding. The advantage of search data is that they can be dedispersed and folded with improved ephemerides at a later time; this allows for iterative improvement of the ephemeris. They also enable the search for pulsations from the neutron star companion (see §3.2), which is not possible with timing data. The disadvantage is that these data have some dispersive smearing, and were not properly flux and polarization calibrated.

Nevertheless, we can estimate an approximate flux density at 1.4 GHz based on the radiometer equation (Dewey et al. 1985) and the PUPPI pulse profile in Fig. 1. Using the characteristics of the L-wide receiver (a gain of 10.5 K/Jy, a bandwidth of 600 MHz, a system temperature of ~ 30 K⁴, to which we add 4 K of background sky temperature) and the characteristics of the detection (total observing time of 5.3 hours, pulse duty cycle of ~ 8 % and signal-to-noise ratio of 98.7) we derive a phase-averaged flux density at 1.4 GHz of $S_{1.4} \sim 0.02$ mJy. For the estimated distance of 7.6 kpc this represents a 1.4 GHz luminosity of $L_{1.4} \sim 1.1$ mJy kpc². More rigorous estimates of flux density, spectral index, scattering times and multi-frequency polarimetric properties of this pulsar will be published elsewhere.

3. Data Analysis and Results

3.1. Timing Analysis

The observations presented in Table 1 were used to derive a timing solution for PSR J1913+1102 using standard pulsar timing techniques (see Lorimer & Kramer 2004, and references therein). First, the data that were obviously affected by radio frequency interference (RFI) were removed; the remaining data were then incoherently dedispersed at $DM = 338.96$ pc cm⁻³ and then folded at the topocentric period of the pulsar. Each of the two ALFA sub-bands were reduced independently and the 600 MHz L-wide band was divided into three 200 MHz sub-bands.

Three standard template profiles were created for the high-frequency ALFA band, the low-frequency ALFA band, and the PUPPI band. These templates were cross-correlated against the corresponding folded profiles to determine pulse times-of-arrival (TOAs) using the “FDM” algorithm of `psrchive`’s `pat` program. The TOAs were fit to a model that accounts for spin, astrometry and binary motion, including the relativistic rate of advance of periastron, $\dot{\omega}$, which was found to be significant. The timing model was fit using `TEMPO`⁵. In fitting the data we used the NASA JPL DE421 Solar System ephemeris (Folkner et al.

⁴<http://www.naic.edu/~astro/RXstatus/rcvrtabz.shtml>

⁵<http://tempo.sourceforge.net/>

2009), and the NIST’s UTC time scale⁶.

The TOAs were split into three sub-sets for the 1) low-frequency ALFA band, 2) high-frequency ALFA band, and 3) L-wide receiver. For each sub-set, the TOA uncertainties were scaled (using an “EFAC” parameter) such that the resulting reduced $\chi^2 = 1$ when the sub-set was fit independently of the others. The multiplicative factors were found to be between 0.89 and 1.0.

The complete fit of all 513 TOAs had a reduced χ^2 of 1.0 and a weighted RMS of the timing residuals of $114 \mu\text{s}$. The fitted and derived timing parameters are shown in Table 2.

3.2. Searching for the Companion of PSR J1913+1102

Given the large mass function for this system, it is likely that the companion of PSR J1913+1102 is another neutron star (see Section 4 for details). If so, then it could in principle be an active radio pulsar, as observed in the J0737–3039 “double pulsar” system. Motivated by this possibility, we have searched for the presence of periodic signals in all available observations with integration times longer than $T \gtrsim 110$ s. This amounts to 11 observations with the central beam of ALFA with $110 \lesssim T \lesssim 1200$ s and 33 observations with the L-wide receiver with durations between ~ 300 s and 1200 s. In all, the observations searched span 1.5 years. Searching data sets with long time spans and covering all orbital phases is important given that pulsars in DNS systems might be eclipsed and/or precess into and out of the line of sight (e.g. Breton et al. 2008).

The low- and high-frequency sub-bands of the Mock Spectrometer ALFA observations were combined and excised of RFI using the methods described in Lazarus et al. (2015). Likewise, several often-corrupted frequency channels were zero-weighted in the incoherent PUPPI observations. RFI masks created with PRESTO’s `rfifind` were applied to the data when dedispersing; after dedispersion we reduce the spectral resolution by a factor of 16, this results in a total of 128 channels. Both raw and zero-DM filtered (see Eatough et al. 2009) dedispersed time series were produced and searched. Binariness was removed from dedispersed time series using the technique described below.

Most of the orbital parameters of the companion’s binary motion are known because the orbit of PSR J1913+1102 has been precisely determined from our timing analysis. The only unknown parameter is the projected semi-major axis of the companion’s orbit, $x_c = a_c \sin i$, where a_c is the semi-major axis of the companion’s orbit and i is the orbital inclination. The

⁶<http://www.nist.gov/pml/div688/grp50/NISTUTC.cfm>

Table 2: Fitted and derived parameters for PSR J1913+1102.

| Parameter | Value ^a |
|--|--------------------|
| <i>General Information</i> | |
| MJD Range | 56072 – 56642 |
| Number of TOAs | 513 |
| Weighted RMS of Timing Residuals (μs) | 114 |
| Reduced- χ^2 value ^b | 1.0 |
| Reference MJD | 56357 |
| Binary Model Used | DD |
| Phase-averaged flux density at 1.4 GHz, $S_{1.4}$ (mJy) | ~ 0.02 |
| Pseudo-luminosity at 1.4 GHz, $L_{1.4}$ (mJy) | ~ 1.1 |
| <i>Fitted Parameters</i> | |
| Right Ascension, α (J2000) | 19:13:29.0542(3) |
| Declination, δ (J2000) | +11:02:05.741(9) |
| Spin Frequency, ν (Hz) | 36.65016488379(2) |
| Spin Frequency derivative, $\dot{\nu}$ ($\times 10^{-16}$ Hz/s) | -2.16(3) |
| Dispersion Measure, DM (pc cm^{-3}) | 338.96(2) |
| Projected Semi-Major Axis, $a \sin i$ (lt-s) | 1.754623(8) |
| Orbital Period, P_b (days) | 0.206252330(6) |
| Time of Periastron Passage, T_0 (MJD) | 56241.029660(5) |
| Orbital Eccentricity, e | 0.08954(1) |
| Longitude of Periastron, ω ($^\circ$) | 264.279(9) |
| Rate of Advance of Periastron, $\dot{\omega}$ ($^\circ/\text{yr}$) | 5.632(18) |
| <i>Derived Parameters</i> | |
| Spin Period, (ms) | 27.28500685251(2) |
| Spin Period Derivative ($\times 10^{-19}$ s/s) | 1.61(2) |
| Galactic longitude, l ($^\circ$) | 45.25 |
| Galactic latitude, b ($^\circ$) | 0.19 |
| Distance (NE2001, kpc) | 7.6 |
| Characteristic Age, $\tau_c = P/(2\dot{P})$ (Gyr) | 2.7 |
| Inferred Surface Magnetic Field Strength, B_S ($\times 10^9$ G) | 2.1 |
| Spin-down Luminosity, \dot{E} ($\times 10^{32}$ ergs/s) | 3.1 |
| Mass Function, f (M_\odot) | 0.136344(2) |
| Total Binary System Mass, M_{tot} (M_\odot) | 2.875(14) |

^aThe numbers in parentheses are the 1- σ , TEMPO-reported uncertainties on the last digit.

^bThe uncertainties of the two ALFA data sets and the L-wide data set were individually scaled such that the reduced χ^2 of the resulting residuals are 1.

ratio of the size of the pulsar’s orbit and the companion’s orbit is related to the unknown mass ratio: $q = M_p/M_c = a_c/a_p$, where M_p and M_c are the pulsar and companion masses, respectively.

Prior to searching for periodicities in the data, each observation was dedispersed at the DM of PSR J1913+1102. The dedispersed time series were transformed to candidate companion rest frames using a custom script that has been incorporated into PRESTO. These were derived for 5000 evenly spaced trial values of companion mass, $M_c \in [1.04 - 2.4] M_\odot$. Then, using the total mass of the system M_{tot} (section 4.2), we calculate the pulsar mass as $M_{\text{tot}} - M_c$. From this we calculate q and x_c . With the rest frame established the dedispersed time series were transformed by adding or removing samples as necessary to keep each sample within 0.5 samples of its corrected value. When a sample is added to the time series its value is set to the value of the preceding sample.

For each of the resulting 5000 time series, the Fast Fourier Transform (FFT) was computed, normalized (including red noise suppression), and searched for un-accelerated signals using 16-harmonic sums. The output candidate lists were sifted through to find promising signals to fold. Significant candidate signals found at the same period in the same observation were grouped together. Likewise, harmonically related candidates were grouped together with the fundamental. The 20 most significant candidates in each observation were folded. Each candidate was folded using the mass ratio at which it was most strongly detected, as well as up to five other mass ratios uniformly distributed over the range of ratios in which the signal was detected. All folding was done with PRESTO’s `prepfold`. Each of the resulting diagnostic plots was inspected manually. The most pulsar-like candidates were compared against a list of known RFI signals from the PALFA survey. Candidates with non-RFI-prone frequencies were re-folded using full radio-frequency information. This procedure was validated by applying it to an observation of the J0737–3039 system. Using the ephemeris for PSR J0737–3039A (Kramer et al. 2006) as a starting point, we were able to detect PSR J0737–3039B.

None of the candidates identified in the search for the companion of PSR J1913+1102 was consistent with coming from an astrophysical source. The minimum detectable flux density of each observation was computed using the radiometer equation, with the same parameters used in Section 2. Because the companion of PSR J1913+1102 would likely be a slow, normal pulsar like PSR J0737–3039B, we did not include the broadening effects of the ISM (DM smearing and scattering) and simply assumed a 5% duty cycle. Furthermore, for simplicity, we did not include the degradation of sensitivity due to red noise found by Lazarus et al. (2015). With these caveats, we derive an upper limit for the 1.4 GHz flux density of about $S_{1.4} < 12 \mu\text{Jy}$ for most of the Mock observations, and $S_{1.4} < 9 \mu\text{Jy}$ for

the longest the Mock observations. For most of the L-wide/PUPPI observations, we obtain $S_{1.4} < 7 \mu\text{Jy}$.

However, in practice these sensitivity limits are not reached in real surveys, where, due to a variety of factors, there is always some sensitivity degradation, especially for slow-spinning pulsars (Lazarus et al. 2015). Not knowing the spin period of the companion of PSR J1913+1102, it is not possible to estimate the degradation factor precisely. If we assume a spin period of the order of a second, as in the case of PSR J0737–3039B, then for DMs of $325 \text{ cm}^{-3} \text{ pc}$, Lazarus et al. (2015) estimate a loss of sensitivity of ~ 2 . Doubling the flux density limit calculated above would translate to a 1.4 GHz luminosity limit of $L_{1.4} < 0.8 \text{ mJy kpc}^2$. This would place the companion among at the lowest 6 % percentile of all pulsars in the ATNF catalog (Manchester et al. 2005) with reported flux densities at 1.4 GHz (PSR J1913+1102 itself is in the lowest 8 % in luminosity).

4. Discussion

4.1. Nature of the companion

Given the orbital parameters of PSR J1913+1102 it is clear its companion is very massive, at least $1.04 M_{\odot}$ (see section 4.2). Therefore, it could be either a massive WD or another NS. For instance, in the case of PSR J1141–6545, a binary pulsar with very similar orbital parameters, the companion to the pulsar is a massive WD (Antoniadis et al. 2011) with a mass of $\sim 1.0 M_{\odot}$ (Bhat, Bailes & Verbiest 2008), which is similar to our lower mass limit for the companion.

However, the measured spin period derivative of PSR J1913+1102 implies a B-field of $2.1 \times 10^9 \text{ G}$ and τ_c of 2.7 Gyr. The characteristic age is much larger, and the B-field is much smaller, than observed for PSR J1141–6545 and the normal pulsar population in general. This implies that, unlike in the case of PSR J1141–6545, PSR J1913+1102 was recycled by accretion of matter from the companion’s non-compact progenitor. During this recycling, the orbit was very likely circularized, as normally observed in all compact X-ray binaries. This means that something must have induced the currently observed orbital eccentricity; the best candidate for this would be the sudden mass loss and the kick that resulted from a second supernova in the system. Thus, the companion is very likely to be another neutron star. Its non-detection as a pulsar could mean that either it is no longer active as a radio pulsar, or that its radio beam does not cross the Earth’s position, or alternatively that it is just a relatively faint pulsar. This situation is similar to all but one of the known DNSs, where a single NS (in most cases the first formed) is observed as a pulsar; the sole exception

is, of course, the “double pulsar” system J0737–3039.

4.2. The most massive DNS known

With the data included in this paper, we have already detected the rate of advance of periastron, $\dot{\omega}$. If we assume this effect to be caused purely by the effects of general relativity (GR) (a safe bet considering the orbital stability of the system and the lack of observation of any variations of the dispersion measure with orbital phase), then it depends, to first post-Newtonian order, only on the total mass of the system M_{tot} and the well known Keplerian orbital parameters (Taylor & Weisberg 1982):

$$\dot{\omega} = 3T_{\odot}^{2/3} \left(\frac{P_b}{2\pi} \right)^{-5/3} \frac{1}{1 - e^2} M_{\text{tot}}^{2/3}. \quad (1)$$

T_{\odot} is one solar mass expressed in units of time, $T_{\odot} \equiv GM_{\odot}c^{-3} = 4.925490947 \mu\text{s}$. The $\dot{\omega}$ observed yields $M_{\text{tot}} = 2.875 \pm 0.014 M_{\odot}$, making J1913+1102 significantly ($0.047 \pm 0.014 M_{\odot}$) more massive than the B1913+16 system, until now most massive DNS known ($M_{\text{tot}} = 2.828 M_{\odot}$; Weisberg & Huang 2016).

It is not yet possible to measure a second PK effect precisely enough to estimate the individual NS masses. However, we can use the known mass function to estimate an upper limit to the pulsar mass ($M_p < 1.84 M_{\odot}$) and a lower limit to the companion mass ($M_c > 1.04 M_{\odot}$, see Fig. 2). These extreme values would occur for an orbital inclination of 90° , i.e., if the system were being seen edge-on.

4.3. The 0.09 clump in orbital eccentricity

The J1913+1102 system is one of the six known DNSs in the Galactic disk that will coalesce in a time shorter than a Hubble time, the others being J0737–3039 (Burgay et al. 2003; Lyne et al. 2004; Kramer et al. 2006), J1906+0746 (van Leeuwen et al. 2015), J1756–2251 (Ferdman et al. 2014), B1913+16 (Weisberg & Huang 2016) and B1534+12 (Fonseca et al. 2014); one of these, J1906+0746, is not securely identified as a DNS. Of these six only J0737–3039 and J1906+0746 have smaller orbital periods than PSR J1913+1102. These three systems have remarkably similar eccentricities: 0.0878 for J0737–3039, $e = 0.0853$ for J1906+0746 and $e = 0.0896$ for J1913+1102.

One question that naturally arises from this similarity is whether this is merely a coin-

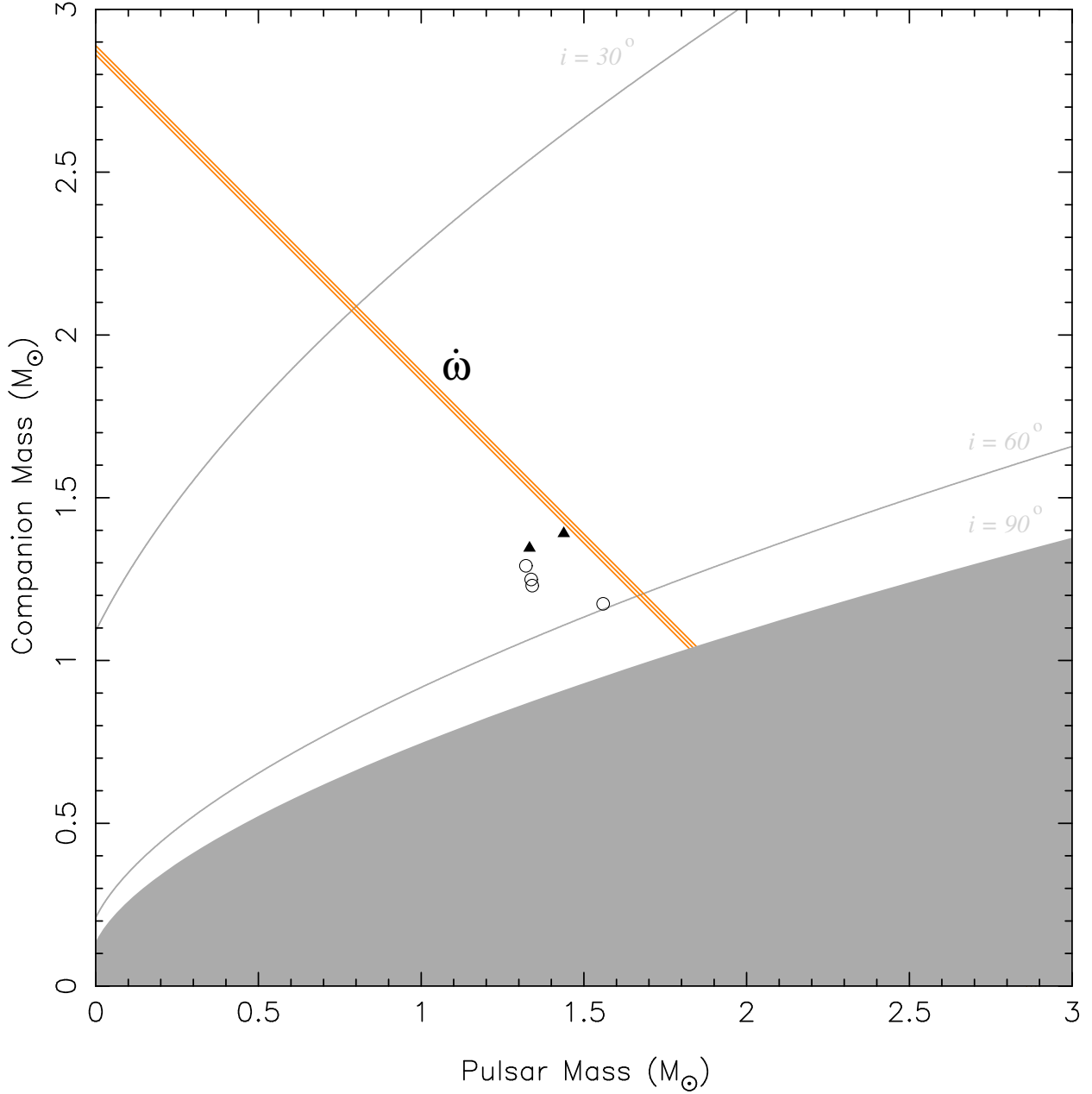


Fig. 2.— Current mass constraints from the timing of PSR J1913+1102. The straight lines correspond to the nominal value and $\pm 1\sigma$ uncertainty of the rate of advance of periastron $\dot{\omega}$. The gray region is excluded by the mass function of the system, and the gray lines indicate constant orbital inclinations of 60° (median) and 30° . The symbols indicate the neutron star masses for DNSs where these have been well measured, the mass of the first formed neutron star is displayed along the x axis. The filled triangles indicate the high-eccentricity DNSs, B1913+16 and B1534+12, the open circles indicate the low-eccentricity DNSs like J1913+1102.

cidence or whether it reflects a deeper similarity between these three systems. One of the features of gravitational wave emission is that it will not only cause a steady decrease in the orbital period of a system, but it will also cause a decrease in the orbital eccentricity with time. This means that, for any group of DNS systems, we will generally see a correlation between orbital period and eccentricity.

In Fig. 3, we see the past and future evolution of e versus P_b for the six aforementioned DNSs, which have short coalescence times. All systems are moving towards smaller e and P_b , i.e., towards the lower left corner.

Regarding the past evolution, we calculate the orbital evolution until a time that is given by the best available proxy for the “age” of the binary, by which we mean the time elapsed since the second supernova. The positions for those initial times are given by the gray-filled points.

In the case of J0737–3039 and J1906+0746 (interestingly, the two systems with the shortest orbital periods), the second-formed NSs are observed as pulsars; their τ_c allow reasonable constraints on the age of the systems. For J0737–3039, the age of the system is either ~ 80 or 180 Myr (Lorimer et al. 2007); for the sake of argument we use the lower estimate. At that time e was about 0.114. For J1906+0746, the young pulsar (the only one detectable in that system) has $\tau_c \sim 100$ Kyr; this number is so small that even if the true age of the system were larger by one order of magnitude, there was just no time for significant change in the orbital eccentricity. Therefore, its current eccentricity is very similar to the orbital eccentricity right after the formation of the second NS.

For the other DNSs, including J1913+1102, we do not currently detect the young pulsars, so we must rely on the τ_c of the recycled pulsars. In the case of J0737–3039, PSR J0737–3039A has $\tau_c = 200$ Myr (Lyne et al. 2004), which is larger than the age estimated from the spin-down of PSR J0737–3039B; the same will likely be the case for the other systems. For PSR J1913+1102, $\tau_c = 2.7$ Gyr; projecting the orbital parameters that far in the past we obtain upper limits for e and P_b of 0.19 and 10.5 hours respectively. Not knowing the τ_c of the second-formed NSs, we can’t derive better constraints on the birth parameters for J1913+1102 and most other DNSs (although in the cases of B1534+12 and J1751–2251, they were likely similar to their current parameters).

Nevertheless, the disparity between the initial orbital eccentricities of J0737–3039 and J1906+0746 and the poorly constrained initial e for J1913+1102 do not positively suggest the existence of a tight clump of orbital eccentricities at ~ 0.09 for the DNSs with the shortest orbital periods.

Looking towards the future evolution of J1913+1102, the system will coalesce in ~ 0.5 Gyr.

These numbers are not yet very precise because we do not yet know the individual masses. In this calculation we use the values in the discussion below ($M_p \sim 1.65 M_\odot$ and $M_c \sim 1.24 M_\odot$); the coalescence time does not change much for a more symmetric system.

4.4. What do the low eccentricities mean?

The observed DNS eccentricities nevertheless show that most of the compact systems have low eccentricities, in marked contrast to B1913+16. After the discovery of J0737–3039, van den Heuvel (2004) pointed out that in the eccentric DNS systems (B1913+16 and B1534+12) the second-formed NSs have masses of 1.389 and 1.346 M_\odot and the systems have high proper motions, while for the low-eccentricity systems (at the time J0737–3039, and now also including J1756–2251 and J1906+0746) the second-formed NSs have masses in the range 1.23–1.29 M_\odot , and at the time no detectable proper motions; this is consistent their location near the Galactic plane despite their large ages. The masses observed in the J1141–6545 system are consistent with the latter scenario: the pulsar formed *after* its heavy WD companion, but it has a relatively low mass of 1.27 M_\odot , and the post-SN orbital eccentricity of the system is 0.17.

All of this is believed to reflect the bimodal nature of the supernovae (SNe) that formed the second NS, with one group of SNe, those that form lighter NSs, having much smaller kicks and associated mass loss. These are thought to be the result of ultra-stripped SNe, which can either be electron capture or iron core-collapse SNe (Tauris et al. 2013, 2015).

Since then, the small kick of the second SN has been confirmed in studies of two low-eccentricity DNSs: The proper motion of J0737–3039 has been measured (Deller et al. 2009); the tangential space velocity v_t was been found to be $\sim 10 \text{ km s}^{-1}$, much smaller than observed for other pulsars and also small compared to the general population of recycled pulsars (for J1756–2251 the limits are not so constraining, $v_t < 68 \text{ km s}^{-1}$, see Ferdman et al. 2014). Furthermore, neither PSR J0737–3039A (Ferdman et al. 2013) nor PSR J1751–2251 (Ferdman et al. 2014) show any changes in their pulse profiles as a result of geodetic precession. The likely reason is the following: after these pulsars were spun up by material from the companion, their spin angular momentum was closely aligned with the orbital angular momentum of the system. After the second SN, its small kick produced only a small change in the orbital plane of the system; therefore the spin angular momentum of these pulsars continues to be closely aligned with the orbital angular momentum. In the case of PSR J0737–3039A, the angle between spin axis and orbital angular momentum is smaller than 3° (Ferdman et al. 2013); for PSR J1756–2251, this angle is smaller than 17° (Ferdman et al. 2014). This implies that, as it precesses around the total angular momentum

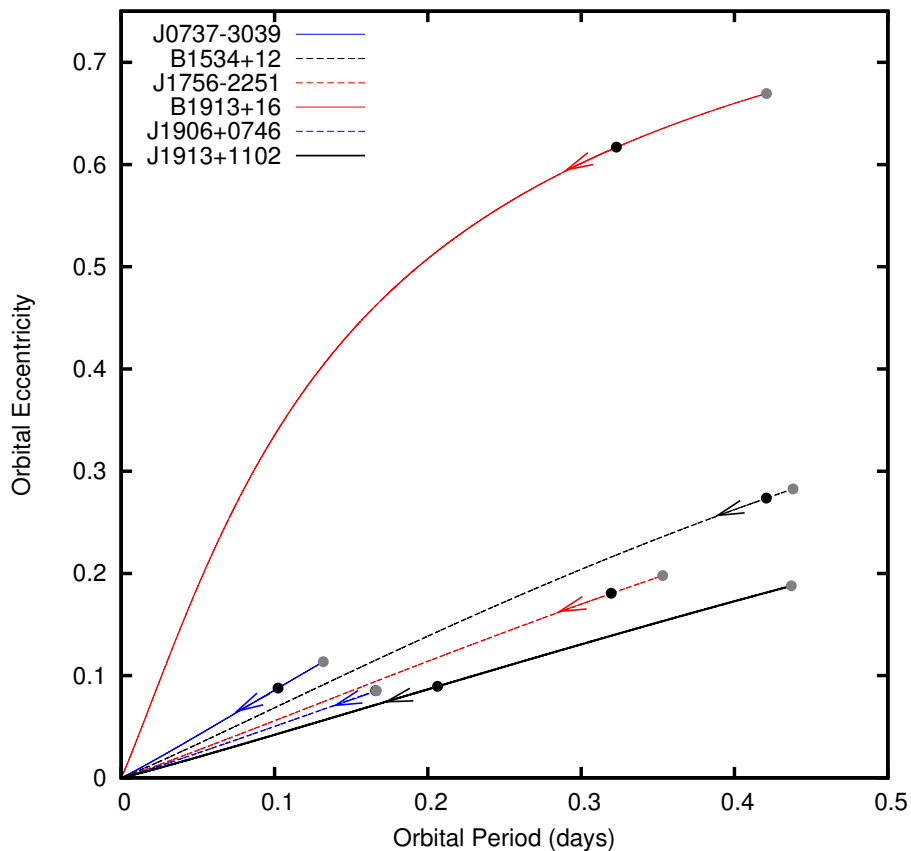


Fig. 3.— Past and future orbital evolution of a set of 6 DNSs, which will coalesce within a Hubble time. Because of orbital energy loss due to emission of gravitational waves, all systems are moving to the lower left corner, with ever smaller orbital periods and orbital eccentricities, reaching coalescence at the origin of the plot. The current positions are given by black dots; our best estimates of the positions right after the second SN are given by gray dots.

of the system, the spin axis of the pulsar will only change direction slightly, resulting in undetectably small changes in the radio pulse profile as observed from the Earth.

Since the SN kick does not influence the inclination, it also has a limited influence on the post-SN eccentricity of the orbit. The small orbital eccentricities in these systems are in large part due to the sudden loss of the NS binding energy (as neutrinos) during the second supernova, see e.g. Bhattacharya & van den Heuvel (1991).

Like the latter systems, J1913+1102 has a low eccentricity and is also located near the Galactic plane ($b = 0.19^\circ$) despite its large age; both of these are consistent with a second SN having a small kick. In this case, we should expect, by analogy with what was said above, that: a) A small peculiar velocity and resulting small proper motion, b) No observation of changes in the pulse profile of the recycled (first formed) pulsar due to geodetic precession, as for PSR J0737–3039A and PSR J1756–2251, and c) The mass for the NS companion to PSR J1913+1102 should be similar to those observed among the second-formed NSs in the the “low-kick” systems, i.e. in the range $1.23–1.29 M_\odot$ (Ferdman et al. 2014; van Leeuwen et al. 2015). All of these characteristics will be determined precisely with continued timing of the pulsar.

5. Prospects

If the prediction of a low-mass companion to PSR J1913+1102 is confirmed, then the system must be very asymmetric: its total mass would imply $M_p \sim 1.65 M_\odot$, and thus $q \sim 1.35$. This might appear to be unusual, but a similarly asymmetric DNS system has already been observed, J0453+1559, where $M_p = 1.559(5) M_\odot$, $M_c = 1.174(4) M_\odot$ and $q = 1.33$ (Martinez et al. 2015). As for all the other compact DNSs, continued timing of PSR J1913+1102 should allow the measurement of a second post-Keplerian parameter, the Einstein delay (γ), and allow a measurement of the individual NS masses in this system.

A mass ratio q larger than 1.3 leads to a peculiar behavior during NS-NS mergers: the lighter (and larger) NS is tidally disrupted by the smaller, more massive NS. According to recent simulations (Rezzolla et al. 2010; Hotokezaka et al. 2013; Rosswog 2013), such mergers result in a much larger release of heavy r-process elements (Just et al. 2015), possibly explaining the heavy element abundances in our Galaxy. However, until now it was impossible to verify whether this scenario happens in the Universe because no asymmetric DNSs are known that might coalesce in a Hubble time. It is therefore very important to determine whether J1913+1102 is really as asymmetric as the above arguments suggest.

As observed in the other compact DNS systems, long-term timing will also result in

the precise measurement of another post-Keplerian parameter, the orbital decay due to the emission of gravitational waves (\dot{P}_b). A measurement of the proper motion will be necessary to ascertain to what degree can we correct for kinematic effects to the orbital decay of J1913+1102 and test the GR prediction for \dot{P}_b . If the pulsar is co-moving with the local standard of rest, we expect a proper motion of about 6 mas/yr. In that case, the contributions from the Shklovskii effect (Shklovskii 1970) will cancel the contribution from differential Galactic acceleration (Damour & Taylor 1991; Reid et al. 2014) for a wide range of distances around the estimated DM distance, 7.65 kpc. If the proper motion is much larger then a precise measurement of the distance will be necessary for a precise test of the radiative properties of gravity. Such a precise distance measurement is unlikely given the low flux density of the pulsar and the large estimated distance.

As mentioned above, this system will coalesce within 0.5 Gyr. With this coalescence timescale, it is unlikely that this discovery will have a large impact on the estimated rate of NS-NS merger events detectable by ground-based gravitational wave detectors. However, if the mass asymmetry is confirmed, it will be important for estimating the rate of events where tidal disruption of a NS is observable.

6. Conclusions

We have presented the discovery and timing of PSR J1913+1102, a 27.3-ms pulsar in a binary orbit with a neutron star companion found in the PALFA survey. Searches of 44 observations for periodic signals from the companion did not result in a detection. A timing analysis of ~ 1.5 yr of data provided a detection of the rate of advance of the periastron of the orbit, which, assuming GR, resulted in a measurement of the total binary system mass of $M_{\text{tot}} = 2.875(14) M_{\odot}$, making this the most massive DNS system known. A comparison of J1913+1102 and other DNS systems suggest that its companion may be a low-mass NS formed via an ultra-stripped SN; in this case the system would be very asymmetric. This possibility will be tested by the end of 2016 by the detection of additional PK parameters.

We thank all Einstein@Home volunteers, especially those whose computers found PSR J1913+1102 with the highest statistical significance: Uwe Tittmar, Kressbronn, Germany, and Gerald Schrader, San Diego, USA. This work was supported by the Max Planck Society and by NSF grants 1104902, 1105572, and 1148523.

The Arecibo Observatory is operated by SRI International under a cooperative agreement with the National Science Foundation (AST-1100968), and in alliance with Ana G. Méndez-Universidad Metropolitana, and the Universities Space Research Association. We

thank all the dedicated staff that work at Arecibo, without their efforts and professionalism this discovery would have been impossible.

Computations were made on the supercomputer Guillimin at McGill University, managed by Calcul Québec and Compute Canada. The operation of this supercomputer is funded by the Canada Foundation for Innovation (CFI), NanoQuébec, RMGA and the Fonds de recherche du Québec - Nature et technologies (FRQ-NT).

PL acknowledges the support of IMPRS Bonn/Cologne. PL, PCCF, and LGS gratefully acknowledge financial support by the European Research Council for the ERC Starting Grant BEACON under contract no. 279702. JSD was supported by the NASA Fermi Guest Investigator program and by the Chief of Naval Research. JWTH acknowledges funding from an NWO Vidi fellowship and ERC Starting Grant “DRAGNET” (337062). JvL acknowledges funding from the European Research Council under the European Union’s Seventh Framework Programme (FP/2007-2013) / ERC Grant Agreement n. 617199. Pulsar research at UBC is supported by an NSERC Discovery Grant and by the Canadian Institute for Advanced Research. V.M.K. receives support from an NSERC Discovery Grant and Accelerator Supplement, from NSERC’s Herzberg Award, from an R. Howard Webster Foundation Fellowship from the Canadian Institute for Advanced Study, the Canada Research Chairs Program, and the Lorne Trottier Chair in Astrophysics and Cosmology.

This research has made use of NASA’s Astrophysics Data System Bibliographic Services.

We also thank the anonymous referee for suggestions that have improved this work.

REFERENCES

- Abadie, J., et al. 2010, *Classical and Quantum Gravity*, 27, 173001
- Allen, B., et al. 2013, *ApJ*, 773, 91
- Antoniadis, J., Bassa, C. G., Wex, N., Kramer, M., & Napiwotzki, R. 2011, *MNRAS*, 412, 580
- Bhat, R., Bailes, N. & Verbiest, J. 2008, *Phys. Rev. D*, 77, 124017
- Bhattacharya, D., & van den Heuvel, E. P. J. 1991, *Phys. Rep.*, 203, 1
- Breton, R. P., et al. 2008, *Science*, 321, 104
- Burgay, M., et al. 2003, *Nature*, 426, 531

- Cordes, J. M., et al. 2006, ApJ, 637, 446
- Damour, T., & Taylor, J. H. 1991, ApJ, 366, 501
- Deller, A. T., Bailes, M., & Tingay, S. J. 2009, Science, 323, 1327
- Dewey, R. J., Taylor, J. H., Weisberg, J. M., & Stokes, G. H. 1985, ApJ, 294, L25
- Eatough, R. P., Keane, E. F., & Lyne, A. G. 2009, MNRAS, 395, 410
- Ferdman, R. D., et al. 2013, ApJ, 767, 85
- Ferdman, R. D., et al. 2014, MNRAS, 443, 2183
- Folkner, W. M., Williams, J. G., & Boggs, D. H. 2009, Interplanetary Network Progress Report, 178, 1
- Fonseca, E., Stairs, I. H., & Thorsett, S. E. 2014, ApJ, 787, 82
- Hotokezaka, K., Kiuchi, K., Kyutoku, K., Muranushi, T., Sekiguchi, Y.-i., Shibata, M., & Taniguchi, K. 2013, Phys. Rev. D, 88, 044026
- Just, O., Bauswein, A., Pulpillo, R. A., Goriely, S., & Janka, H.-T. 2015, MNRAS, 448, 541
- Kramer, M., et al. 2006, Science, 314, 97
- Lattimer, J. M., & Prakash, M. 2004, Science, 304, 536
- Lazarus, P., et al. 2015, ApJ, 812, 81
- Lorimer, D. R., et al. 2007, MNRAS, 379, 1217
- Lorimer, D. R., & Kramer, M. 2004, *Handbook of Pulsar Astronomy* (Cambridge University Press)
- Lorimer, D. R., et al. 2006, ApJ, 640, 428
- Lyne, A. G., et al. 2004, Science, 303, 1153
- Martinez, J. G., et al. 2015, ApJ, 812, 143
- Manchester, R. N., Hobbs, G. B., Teoh, A., & Hobbs, M. 2005, AJ, 129, 1993
- Reid, M. J., et al. 2014, ApJ, 783, 130

- Rezzolla, L., Baiotti, L., Giacomazzo, B., Link, D., & Font, J. A. 2010, *Classical and Quantum Gravity*, 27, 114105
- Rosswog, S. 2013, *Philosophical Transactions of the Royal Society of London Series A*, 371, 20120272
- Shklovskii, I. S. 1970, *Soviet Ast.*, 13, 562
- Tauris, T. M., Langer, N., Moriya, T. J., Podsiadlowski, P., Yoon, S.-C., & Blinnikov, S. I. 2013, *ApJ*, 778, L23
- Tauris, T. M., Langer, N., & Podsiadlowski, P. 2015, *MNRAS*, 451, 2123
- Taylor, J. H., & Weisberg, J. M. 1982, *ApJ*, 253, 908
- van den Heuvel, E. P. J. 2004, in *ESA Special Publication*, Vol. 552, 5th INTEGRAL Workshop on the INTEGRAL Universe, ed. V. Schoenfelder, G. Lichti, & C. Winkler, 185
- van Leeuwen, J., et al. 2015, *ApJ*, 798, 118
- Weisberg, J. M., & Huang, Y. 2016, arXiv:1606.02744